(Figure 5). This configuration resulted in some bending stresses in the brace due to the wet concrete, but there was additional support added and the stresses were insignificant. A 5,000 psi compressive strength, self consolidating concrete mix was used. The braces were moved after three days and installed when the concrete reached about 75% of the design strength.

FIGURE 5 – CONCRETE BEING PLACED INSIDE CFT VERTICAL BRACE

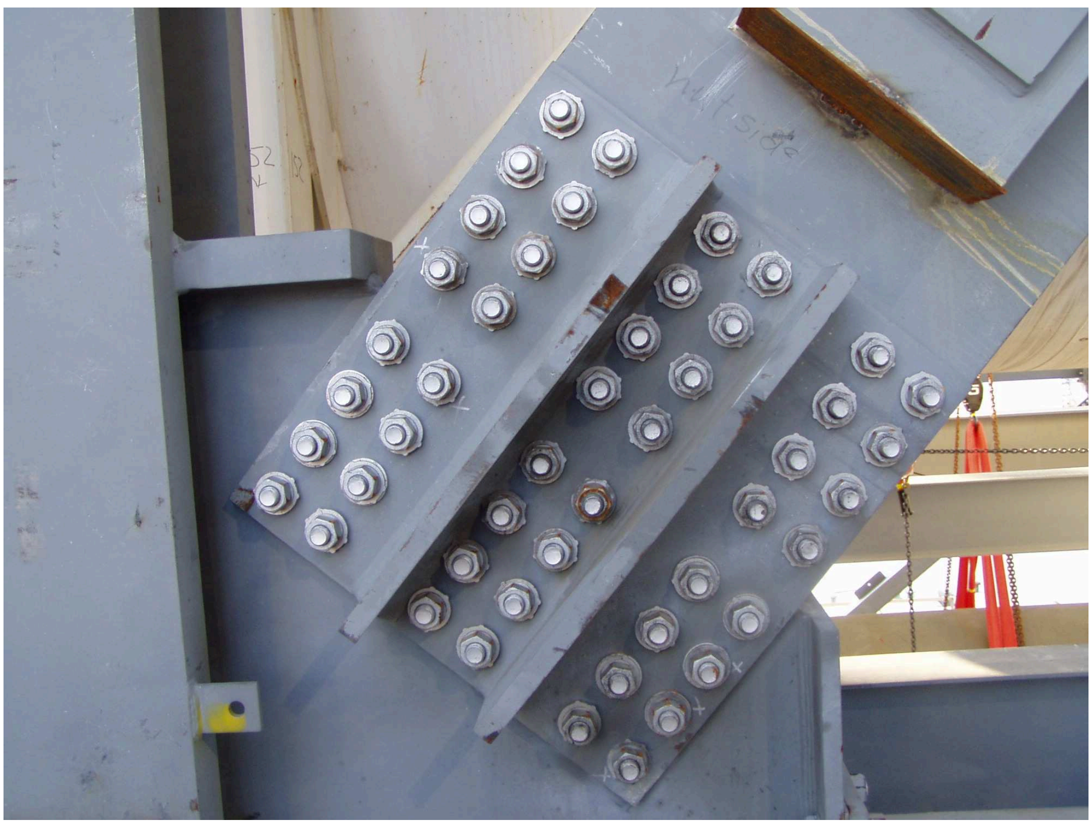

FIGURE 6 – TYPICAL INSTALLED CONNECTION AT CFT VERTICAL BRACE

FIGURE 7 – MULTIPLE CFT VERTICAL BRACES AT A COLUMN/BEAM INTERSECTION

REFERENCES

[1] American Institute of Steel Construction, "Seismic Provisions for Structural Steel Buildings", AISC 341-02, May 21, 2002.

[2] International Code Council, "International Building Code 2003".

[3] American Institute of Steel Construction, "Load and Resistance Factor Design Specification", December 27, 1999.

From Cooling Towers to Chimneys of Solar Upwind Power Plants

Authors:

Reinhard Harte, Bergische Univerity Wuppertal, Pauluskirchstrasse 7, D-42285 Wuppertal
Wilfried B. Krätzig, Ruhr-University, D-44780 Bochum
Hans-Jürgen Niemann, Ruhr-University, D-44780 Bochum, hans-juergen.niemann@rub.de

Natural Draft Cooling Towers as Solar Chimney Protagonists

Natural draft cooling towers and chimneys of solar updraft power plants have many structural properties in common: They are dominated by thin ring-stiffened shell structures made of reinforced concrete, they transport by their internal updraft warm air into the atmosphere, and because of their height, gale actions play the most important role in the design.

Natural draft cooling towers (NDCT) serve in electricity generation in steam power plants for increase of the total degree of efficiency and for an environmentally compatible release of the residual process heat [Gould 2004]. Their principal purpose thereby is the permanent accomplishment of a heat sink at the steam turbines' (cold) ends by providing cooling water for use in the condenser. Therein this water is warmed-up and then re-cooled by dripping from the water distribution of a cooling tower down to the water basin, collected there for re-use in the condenser. This process releases heat inside the tower, and the difference in density of the warm air inside and the colder air outside the tower creates the natural draft. This upward flow of warm air, leading to a continuous stream of fresh air through the air inlets into the tower, is protected against atmospheric wind by the huge RC shell, which forms the characteristic views of NDCTs. Figure 1 shows the presently world highest cooling tower shell. With a height of 200 m, the tower belongs to the 960 MW RWE lignite Power Station at Niederaussem, situated west of Cologne/Germany. The reader may observe its considerably thin RC wall, with thicknesses from 22 cm to 27 cm above the lower lintel [Busch et al 2002]. Figure 2 shows the power block under construction in 2001, besides older power blocks in service.

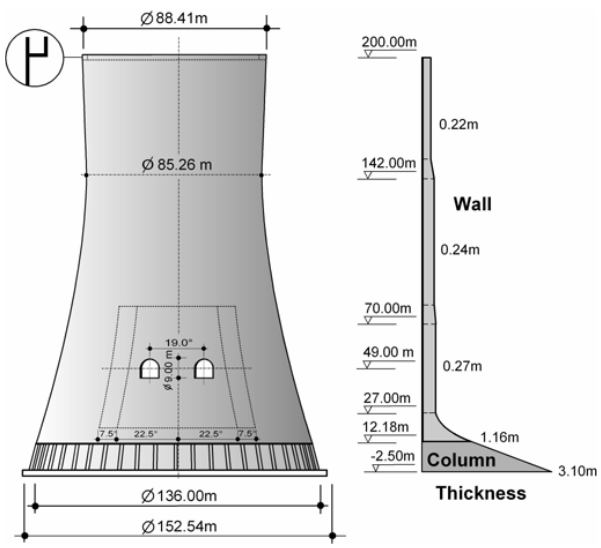

FIGURE 1 - COMPONENTS AND DIMENSIONS OF THE 200M NDCT AT NIEDERAUSSEM POWER STATION

Chimneys of solar chimney power plants (SCPP) also transport warm air to the atmosphere, heated in the glass-covered collector by solar irradiation. This mass-stream of warm air produces electric energy in turbo-generators, located at the foot of the chimney. Such structures also consist of thin RC shells, with intermediate rings, as the feasibility study in figure 2 points out. The air temperature is higher than in NDCTs. For economic reasons, the chimneys reach enormous heights, at least compared to cooling towers [von Backström et al 2008].

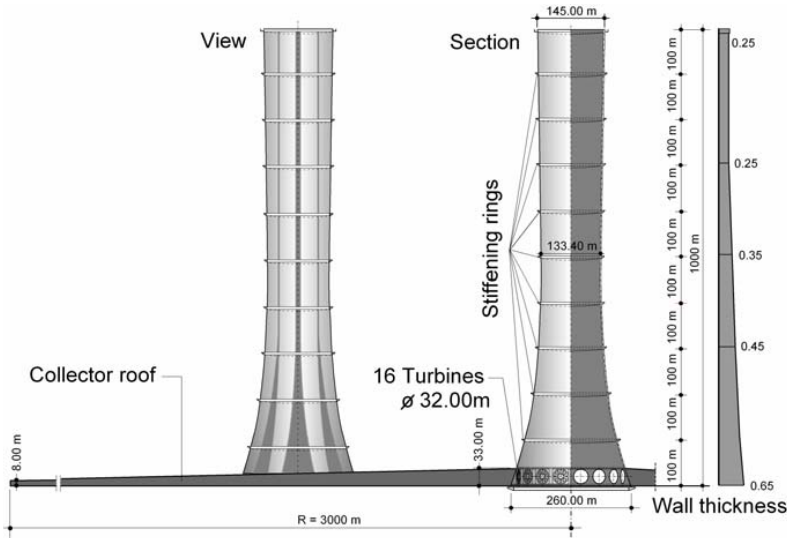

FIGURE 2 - 1000 M CHIMNEY FOR A 200 MWP SCPP

Components and working principle of a Solar Chimney Power Plant

The general working concept of a SCPP is illustrated in figure 3. Such power plant consists of the collector area (CA), the turbine(s) with coupled generator(s) as power conversion unit (PCU), the solar chimney (SC) and the electrical equipment (EQ). In the CA, a large glass-covered area, wide-banded solar UV irradiation heats the collector ground, changes there to IR-radiation, and consequently warms up the bottom air inside the CA. Following the increasing height of the roof, the heated air streams towards the chimney at the collector centre, and fresh cold air is drawn into the CA at its perimeter slot. In the PCU at the SC foot, the mass stream of warm air is transformed into kinetic and further into electric power. For increased effectiveness, a pressure sink at the PCU's outlet is created by the huge SC releasing the air into greatest possible height. For all details of the complex irradiation transmission, repeated reflection and final air-absorption - processes of real Hi-Tec - see [von Backström et al 2008, Pretorius et al 2007, Pretorius 2007]. The driving force that causes the heated air to deliver work in the PCUs and then flow through the SC is the difference in weight between a column of cold air outside and of warm air inside. Obviously, the potential of a SCPP depends on the difference in air temperature, and on the height of the tower.

Solar updraft power plants are the most sustainable natural resources for electric power generation. During service, they are completely free of carbon-dioxide emissions, since they use solar irradiation as fuel. If one incorporates all materials required for the plant construction in an energy balance, measured by CO_2-emissions, one ends up with around ≈10 g of CO_2 per kWh of produced electric work, depending on the service life-duration of the plant. Since design service-lives are 80 to 120 years, CO_2-emissions and production costs of the electric current are by far the smallest ones of all renewable energies, even if a renewal of the turbo-generators and parts of the glass-roof are included. SCPPs will demonstrate their efficiency in areas with solar irradiation of above 2.2 MWh/a, e.g. in all deserts up to 30° latitude north and south of the equator. The degree of efficiency of a SCPP then depends primarily on the size of the CA (air temperature) and on the height of the SC (pressure difference) [Schlaich 1995]: A CA-diameter of 7.000 m and a SC-height of 1.500 m will deliver a maximum electric power of around 400 MWp, on summer mid-days.

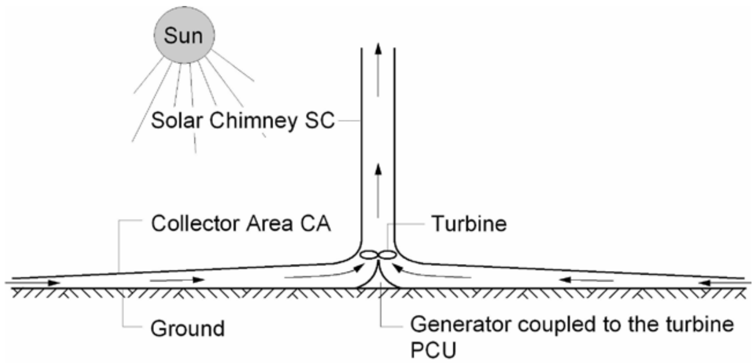

FIGURE 3 - SCHEMATIC WORKING PRINCIPLE OF A SCPP

Such solar updraft power generation has first been proposed in 1903 by the Spanish engineer I. CABANYES, followed by a description of the German scientist [Günther 1931]. Around 1975, several patents were granted to the US engineer R.E. LUCIER in countries with deserts suitable for SCPPs, like Australia, Israel and the US. Starting in 1982, a team with the German civil engineer J. SCHLAICH constructed a prototype SCPP in Manzanares/Spain, with a 200 m high SC and a maximum power output of 50 kW. This prototype plant operated successfully for more than 6 years; and created basic figures for all future developments. Since those days, several projects for SCPPs have been planned in the world's arid zones, but none of them has been brought to realization, up to now.

The Manzanares prototype plant contained a single PCU with vertical turbine axis. Such solutions have been discussed also for bigger plants, but modern designs like in Figure 2 show series of CPUs with horizontal axes around the tower foot perimeter, an arrangement more advantageous for turbine installation, machine control, and maintenance, and - last but not least - efficiency of energy output.

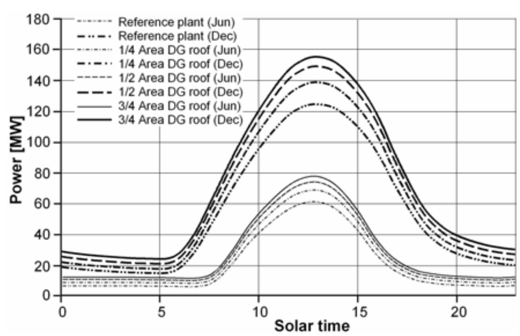

FIGURE 4 - TYPICAL DAILY POWER OUTPUT PROFILE OF A SCPP; DG - DOUBLE GLAZED

Figure 4 illustrates typical daily power output profiles from summer to winter time (southern hemisphere) of a typical large SCPP. One observes that this type of power plants provides certain daily storage capacities, since it also delivers electric power during night hours. Such storage capacity can be extended by arranging passive storage devices, like water-filled black rubber containments in the CA.

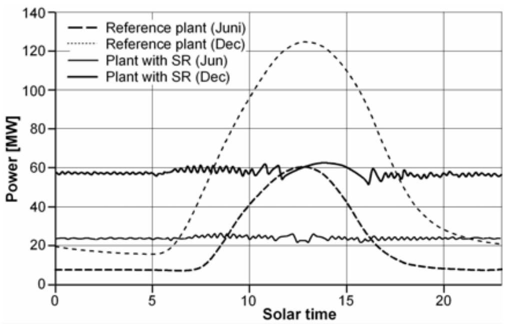

FIGURE 5 - BASE-LOAD SERVICE OF A SCPP WITH DOUBLE GLAZED CA AND SECONDARY ROOF (SR)

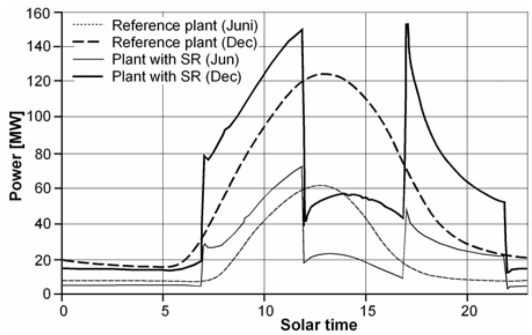

FIGURE 6 - PEAK-LOAD SERVICE OF A SCPP WITH DOUBLE GLAZED CA

Actively controlled storage properties can be formed by double glazed parts of the CA, from which the stored heat can be worked-off either from the upper or the lower compartment or from both, leading to base-load supply service characteristics, as Figure 5 demonstrates. In Figure 6 we observe, that also peak-load services can be offered by SCPPs, all making the electric power from these plants much more valuable than from all other renewable sources. Many further details can be found in [Pretorius et al 2006].

Solar chimney: The dominant role of storm actions

Solar chimneys as dominant structures of SCPPs are subjected to typical actions:

- Dead weight D, mainly from the self-weight of the shell wall (25.0 kN/m³);
- Wind loading W consisting of the external pressure distribution and the internal suction;
- Dynamic along wind load due to wind gustiness, and cross wind loading caused by regular periodic vortex separation;
- Temperature effects T from actions, of the heated air on the RC wall;
- Shrinkage effects S in the (fresh) RC shell may lead to cracking by residual stress states;
- Differential soil settlements B of external origin;
- Seismic actions E, if the location of the SCPP owns a sufficient seismicity;
- Construction loads M mainly from pre-stressed guys of the central tower crane.

From all these actions, wind effects play the most important role in the tower design. They dominate largely the tower costs and thus decide on the economic feasibility of the SCPP technology. The wind loads cannot be taken from wind loading standards since such codes are restricted to structures less than 200 m in height, see e.g. the Eurocode for wind actions [EN 1991-1-4], and not applicable to the large SC-towers of 1000 m and more. A specific wind loading model for SCs is therefore required, and outlined briefly in this section.

Design wind speed and partial safety factors. The design wind load is derived from the adequate level of reliability. For example, the Eurocode [EN 1990] "Basis of design" specifies a target maximum of the failure probability of $P_f = 1.25\ 10^{-6}$ related to one year, corresponding to $P_f = 7.2\ 10^{-5}$ in the design working life of 50 yrs. Related values of the minimum reliability index are $\beta = 4.7$ (one year) and $\beta = 3.8$ (50 yrs). All these targets are notional, intended primarily as a tool for developing consistent design rules. The relation between P_f and β is given by $P_f = \Phi(-\beta)$, in which Φ is the standard Gauss probability function. The related probability of exceeding the design value of an action effect, E_d, in the ultimate limit state of structural failure, is somewhat higher and calculated from $P(E>E_d) = \Phi(\alpha_E\beta)$ in which α_E is the participation factor of the load considered, $-1 \leq \alpha_E < 0$. From $P(E>E_d)$, the design wind speed can be calculated from an appropriate extreme value probability function of yearly maxima of mean wind speeds. For practical reasons, the design wind speed is related to a reference, so-called characteristic wind speed which has a return period of 50 yrs. The ratio of design to characteristic wind loads is the partial safety factor. Since the wind load is proportional to the square of the wind speed, the partial wind load factor is the square of the wind speed ratio. The result of this operation depends much on the type of probability distribution fitted to observed statistical wind data. The Eurocode 1990 recommends a partial factor of $\gamma_W = 1.5$ based on the Gumbel type I probability distribution. It is a general factor most non-permanent loads. Applying the procedure to the wind loading problem, it is generally assumed that the Gumbel I distribution applies to the statistics of mean wind speeds. The following table shows the partial wind load factor calculated for different probability functions and participation factors. The first two applications rely on the Gumbel type I distribution.

Type of pdf	α_W	β_1	$\Phi(\alpha_W \cdot \beta_1)$	V_v	γ_W
Gumbel I	-0.7	4.7	$4.5 \cdot 10^{-4}$	0.12	1.5 – 1.6
Gumbel I	-1.0	4.7	$1.25 \cdot 10^{-6}$	0.12	2.0
Gumbel III	-1.0	4.7	$1.25 \cdot 10^{-6}$	0.12	1.4

The first line relates to a case, where the wind load is the leading action amongst others. The partial factor is close to the code specification. The second line is a limiting, rather unrealistic case where all design variables other than the wind load are deterministic. The partial factor will always be lower than this value. The type I distribution has neither lower nor upper limits. Obviously, there must be an upper limit of possible wind speed intensity. The Gumbel type III distribution includes this option. Wind data from ca. 60 meteorological stations all over Germany have been analyzed to estimate the upper limit in relation to the individual mean and standard deviation; [Niemann et al. 2007]. The result of this investigation is a partial factor of 1.4 shown in the third line. It indicates that the standard load factor is on the safe side and may eventually be reduced without any loss in target reliability.

Mean wind and turbulence beyond the Prandtl layer. Prandtl's constant shear concept for boundary layers in fluid dynamics, describes the natural wind flow up to 70 - 100 m distance to the ground correctly. It is adequate for wind loads on structures, extending to a height of up to 300°m. The model subdivides the wind speed into mean and turbulent components. The mean wind profile specifies the mean wind load, whereas the turbulence parameters (intensity, integral length scales as a measure for correlation, and spectral density) provide the input to the dynamic load. Solar chimneys reach far beyond the Prandtl layer into the Ekman layer. Here, the shear and the turbulence decrease, whereas the Coriolis force becomes important. It increases the mean wind speed and diverts the flow from the direction of the isobars according to the so-called Ekman spiral. The difference between gust and mean wind speed vanishes asymptotically as the height above ground increases, see fig. 7. A 1500°m tower approaches even the height of the ABL thickness $z = \delta$, where the ABL ends and the geostrophic wind flow prevails. At $z \geq \delta$, the shear is negligible and the dynamic load component vanishes. In the Ekman layer, experimental meteorological data are scarce. However, theoretical considerations provide adequate models for the mean and fluctuating wind components, see e.g.

[Harris and Deaves 1980]. The model refers strictly to neutral thermal stratification. In non-neutral conditions, downbursts increase the peak gust velocity [Bradbury et al. 1994] and may become important for the collector glass roof. The material properties of the fluid, especially its density $\rho = \rho(z)$ but as well the viscosity, vary over the tower height. At 1500m above ground the mass density is 87% of its value at ground level. The wind load diminishes accordingly.

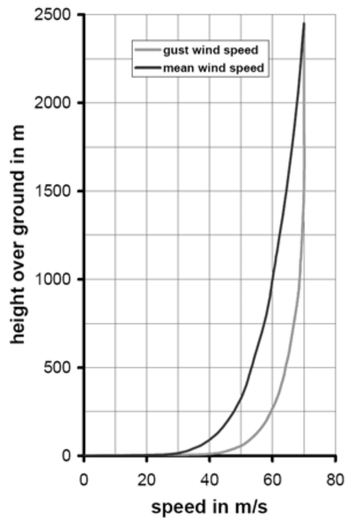

FIGURE 7 – PROFILES OF MEAN AND GUST WIND SPEED

Wind loading. The mean wind load is represented by pressure differences resulting from a uniform negative pressure inside the tower and the external pressure distribution. The latter depend on Reynolds number and on the roughness of the exterior surface. The load distributions developed for NDCTs since the mid 1960s [Niemann 1993] apply also to the Solar Chimney, with two exceptions. (1) In the tip region, the pressures deviate from the typical circumferential distribution observed at lower levels at the tower height. Due to the higher slenderness of SCs compared to NDCTs, this so-called tip effect extends over a larger part of the tower height and must be taken into account. (2) High surface roughness reduces the suction peaks at the tower sides. This effect diminishes the tensile meridional stresses in a NDCT shell. For this reason, wind ribs are commonly applied at the exterior surface of cooling towers. For SCs however, another effect of their higher slenderness is that the stress distribution comes closer to a beam. The stiffening of the SC shell by a number of rings increases this tendency. In such a case, the stresses are smaller with a smooth surface which now becomes the optimal solution for SCs.

The response to wind turbulence has two components: (i) the response to background turbulence which goes without resonance and includes the lack of correlation of the pressure fluctuations on the shell surface; (ii) the resonant response which is caused by turbulence in resonance with vibration modes. The resonant component is small if the natural frequency n of the excited mode is sufficiently high. Then, an overall dynamic amplification factor will suffice to account for resonance. For Solar Chimneys the minimum natural frequency n may be estimated from

$$n > (6/H)^{0.36},$$

in which H is the tower height in m. The rms. pressure fluctuations and their correlations are the basis to calculate the quasi-static shell stresses induced by turbulence. This approach –

called co-variance method [Niemann et al. 1996] – relies on statistical averages obtained from measured time series rather than on the time series themselves. It is preferred here instead of calculating the response in the time domain. Experimental results show that the pressure standard deviations σ_p, are proportional to the turbulence intensity I_v. At stagnation, the coefficient of σ_p / q_m (q_m designates the stagnation pressure of the mean wind speed) is $\sigma_p(z,0) / q_m(z) = 1.8\, I_v(z)$. As fig. 8 shows the intensity of pressure fluctuations varies along the circumference: it is constant before separation and drops to 50% in the wake.

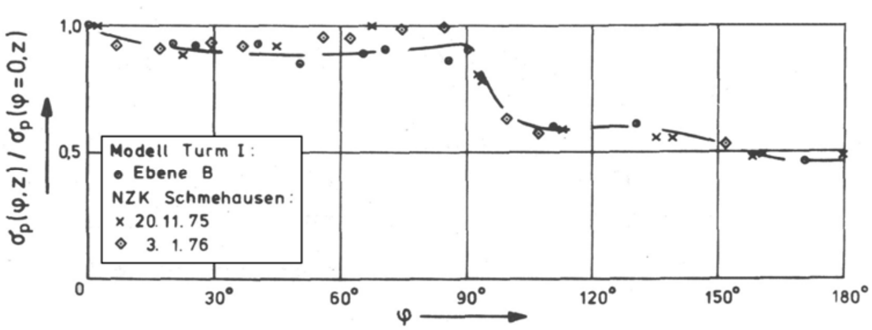

FIGURE 8 - RMS PRESSURE DISTRIBUTION AT LEVEL Z FROM FULL-SCALE MEASUREMENTS AND WIND-TUNNEL EXPERIMENTS

Fig 9 shows pressure correlations along the circumference for various reference points. The correlation between the stagnation point and other points at the circumference reflects the mean flow field: stagnation and maximum suction have strong negative correlation, cith the wake is negative as well but small. Current calculations show that these results strongly affect the magnitude of the response to turbulence. The vertical correlation of pressures at two levels z_1 and z_2 along a meridian is equally important. It depends primarily on the correlation of turbulence. It is usually based on the integral length scale $L_{uz}(z_m)$ at the intermediate level $z_m = (z_1 - z_2)/2$:

$$\rho_z = \exp((z_1 - z_2) / L_{uz}(z_m))$$

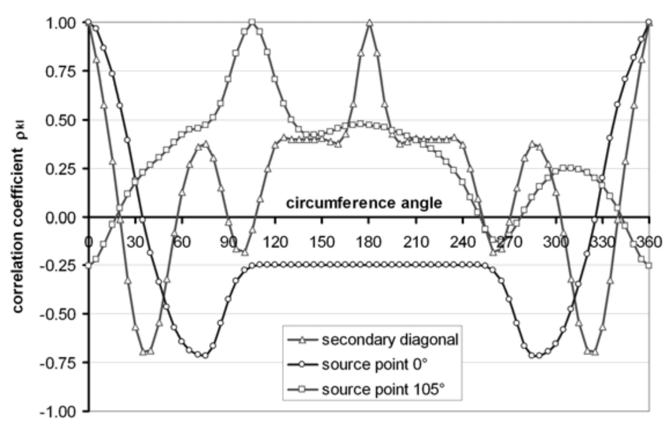

FIGURE 9 - PRESSURE CORRELATIONS ALONG THE CIRCUMFERENCE FOR VARIOUS REFERENCE POINTS